Biogas Upgrading by Transition Metal Carbides

Christian Kunkel, Francesc Viñes,· and Francesc Illas

Departament de Ciència de Materials i Química Fisica & Institut de Química Teòrica i Computacional (IQTCUB), Universitat de Barcelona, Martí i Franqués 1, 08028 Barcelona, Spain

AUTHOR INFORMATION

Corresponding Author

*francesc.vines@ub.edu

Keywords: Transition metal carbides • density functional theory • Biogas upgrading • CO_2/CH_4 separation • Transition state theory

ABSTRACT

The separation of carbon dioxide (CO_2) from methane (CH_4) is critical in biogas upgrading, requiring materials with high selectivity towards one of the two gas components. Hereby we

show, by means of density functional theory based calculations including dispersive forces description, the distinct interaction of CO_2 and CH_4 with most stable (001) surfaces of seven transition metal carbides (TMC; TM = Ti, Zr, Hf, V, Nb, Ta, Mo). Transition state theory derived ad/desorption rates suggest a very high CO_2 uptake and selectivity over CH_4 even at ambient temperature and low partial gas pressures.

Serious concerns about climate change are associated with rising atmospheric concentrations of greenhouse gases like carbon dioxide (CO_2) and methane (CH_4).[1] A reduction of emissions is needed, encouraging the use of renewable energies that contribute in satisfying the worldwide

growing energy demand.[1] Among other available technologies, biogas production from anaerobic digestion is a viable approach,[2] offering a route towards CH_4, an interesting energy source and carrier, obtainable in 50-75 v/v % purity, but admixed with 25-50 v/v % CO_2, which lowers the energy content but in turn allows a direct use in combined heat and power plants (CHPs) after removal of other minor constituents.[3] The use of CH_4 as fuel is to date hampered, requiring a purity > 95 v/v %.[3] Separation of CO_2 while retaining CH_4 in the gas stream is thus a critical step for biogas upgrading,[3] whose concomitant economic and ecologic interest extends to other upgradable sources of CO_2/CH_4 mixtures,[4] *e.g.* landfill and coal mine ventilation airs, and natural gas.

Despite both CO_2 and CH_4 are quite stable and mostly inactive, the noticeable CO_2 quadrupole moment allows for a strong interaction with some privileged materials,[5,6] a factor lacking in the nonpolar CH_4, which weakly interacts with most of them.[7] Thanks to such polarity differences, CO_2/CH_4 efficient separation seems *a priori* possible. However, materials with a high CO_2 selectivity over CH_4 at standard temperature/pressure operation conditions are needed. There is exhaustive experimental research on promising materials,[8] yet performance regretfully often remains low.

Materials screening is conveniently first sieved from simulations accurately estimating the interaction of a given material with CO_2 and CH_4. Among other methods,[7,9] density functional theory (DFT) including dispersion (DFT-D) has proven especially useful to size CH_4 interactions with Ni[10] and Co[11] surfaces, nanoporous carbons,[9] zeolites,[7] periodic mesoporous phenylene-silica (PMOs),[8] and metal organic frameworks (MOFs).[12] Similar examples are available for CO_2,[13] and, in combination with statistical thermodynamics based approaches,

realistic and therefore useful estimates of selectivity and uptake rates are accessible.[8,14]

We recently applied this computational strategy to assess CO_2 capture on most stable and exhibited (001) surfaces of transition metal carbides (TMCs), with 1:1 TM:C ratio and rocksalt crystal structure under standard and moderate pressures.[15] TiC, ZrC, HfC, NbC, TaC, and δ-MoC were TMCs found to strongly adsorb and even activate CO_2 —a noteworthy case of CO_2 chemisorption. This exceptional behavior can allow for CO_2 capture even at ambient temperatures and low gas partial pressure, with the specific storage power dependent on the TMC composition.[13] The CO_2 capture and activation on TMCs, as predicted by DFT, has been previously directly evidenced by infrared spectroscopy and indirectly by its hydrogenation.[16,17] Such reactivity suggest promising usage of TMCs to catalyze a wide variety of reactions,[13,18] often equaling or surpassing Pt group catalysts performance,[19] with the added benefit of low cost, chemical robustness, and poisoning resistance.[18]

Theoretical simulations on CH_4 interaction with TMC surfaces are rather sparse. Only Tominaga *et al.* predicted CH_4 reforming to ethylene on orthorhombic β-Mo_2C surfaces,[20] and a recent DFT-D study showed strong CH_4 physisorption on δ-MoC (001), with a predicted possible methane capture at room temperature.[21] Indeed, molybdenum carbides are known to be very reactive TMCs, and CH_4 adsorption is assumed to be weaker on others. That in mind, TMCs could then be suited for CO_2 removal from mixed CH_4/CO_2 gas streams. To evaluate this possibility, we carried out a thorough DFT-D study of CH_4 attachment to most stable (001) surfaces of seven different TMCs, providing a realistic estimate of initial CO_2/CH_4 selectivity. As done in previous works,[13] we restrain our study to experimentally known rocksalt TMCs with 1:1 TM:C ratio, known to be the stable phase under standard and moderate pressure and

temperature conditions.[15] Thus structural aspects are circumvented and a meaningful comparison is feasible, while including group 4 (TiC, ZrC, and HfC), group 5 (VC, NbC, and TaC), and group 6 (δ-MoC) TMCs. Note that for MoC rocksalt packing is only present in the high temperature δ-phase.

To assess the CH_4 adsorption on the different TMCs, periodic DFT based calculations were carried out on suitable surface models using the Vienna *Ab Initio* Simulation Package – VASP code.[22] The Perdew-Burke-Ernzerhof (PBE)[23] exchange-correlation (xc) functional was used to account for xc effects, to which the dispersion (van der Waals) correction D3 as proposed by Grimme (PBE-D3)[24] was added. Further computational details are found in the Supporting Information. For the sake of the oncoming discussion clarity it is necessary to state that favourable adsorption energies, E_{ads}, are defined negative.

First, the surface exposed sites that most strongly interact with CH_4 have been identified by a computational screening at PBE-D3 level: Four non-equivalent sites were tested for each TMC (001) model, namely bridge Mo-C (b), hollow (h), top C (t^C) and top metal (t^M). Interaction at each site was evaluated with two different CH_4 orientations, with either two or three H pointing towards the surface, denoted H_2 and H_3, respectively.[21] Notice that orientations with a sole H pointing towards the TMC surface were neglected as previously found to be overall less favourable.[21] Results show that all optimized structures yield rather similar E_{ads} within a range of 0.1 eV. Still, $H_2(t^M)$, $H_3(b)$, and $H_3(t^M)$ lead to most favourable adsorptions for all considered TMCs, to which further assessment is focused onto. The corresponding PBE-D3 adsorption energies are reported in Table 1. Results show that adsorption on TiC, ZrC, HfC (group 4) and VC, NbC, TaC (group 5) is favourable at PBE-D3 level, with E_{ads} values ranging -0.19 to -

0.23 eV, and well agreeing to DFT-D results on other materials, *e.g.* -0.19 eV on Ni (110) and (100) surfaces,[10] or -0.12 eV on MgO (001).[25]

Table 1. PBE-D3 adsorption energies, E_{ads}, of CH_4 on TMC (001) surfaces. Previously reported values for adsorbed CO_2 are also included.[13] All values are given in eV.

E_{ads}	CH_4			CO_2	
	$H_2(t^M)$	$H_3(b)$	$H_3(t^M)$	MMC	TopC
TiC	-0.23	-0.23	-0.23	-0.81	-0.83
ZrC	-0.23	-0.23	-0.23	-1.56	-1.60
HfC	-0.23	-0.23	-0.23	-1.62	-1.65
VC	-0.21	-0.22	-0.21	-0.19[b]	-0.04[b]
NbC	-0.19	-0.19	-0.19	-0.87	-0.70
TaC	-0.23	-0.23	-0.21[a,c]	-1.21	-0.94
δ-MoC	-0.77	-0.77[a]	-0.76	-1.20	-1.03

[a] Spurious imaginary frequencies found, see main text and Supporting Information.
[b] More stable physisorbed E_{ads} of -0.28 eV was used for rate evaluation.
[c] Minor convergence problems occurred, see discussion in Supporting Information.

Methane adsorption is almost exclusively due to dispersive forces, as revealed by comparing to PBE values, see Table S1 in the Supporting Information, where adsorption energies range +0.03 to -0.02 eV, suggesting that the electronic interaction in between CH_4 and TMC surfaces is almost negligible. Given the weak interaction neither significant distortion of CH_4 nor of surface atoms is found. CH_4 is adsorbed ranging 3.06 to 3.39 Å away from the surface, distance measured by the vertical distance between methane carbon and highest surface carbon, see Fig. 1 and distances in Table S1 of the Supporting Information. Altogether, CH_4 interaction on TMCs (001) surfaces can be safely related to physisorption. The δ-MoC case is to

be discussed apart; E_{ads} values are of the order of ~-0.8 eV, and so significantly higher compared to the rest of studied TMCs, and actually also electronically favored since PBE E_{ads} values contribute ~-0.55 eV.[21]
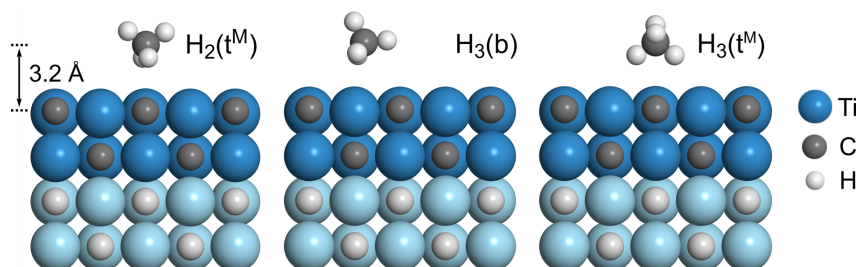

Figure 1. Side sketches of CH₄ adsorbed on TiC (001) in the three different considered cases. Lighter color layers were fixed during optimization. For top views of all geometries, see Supporting Information.

With results for methane interaction laid out, a straight comparison to earlier results for CO_2 adsorption[22] allows a first assessment of selectivity. CO_2 was found to adsorb strongly on two sites, namely MMC and TopC, see their PBE-D3 adsorption energies in Table 1. Direct comparison already suggests a high CO_2 selectivity over CH_4 for few TMCs (TM = Ti, Zr, Hf, Nb, Ta): Adsorption energies for CH_4 are on the order of ~-0.2 eV, while values for CO_2 exceed these by 3.5 to 8 times, ranging from ~-0.7 to ~-1.6 eV depending on the TMC. On δ-MoC both CH_4 and CO_2 adsorptions are rather strong; selectivity is therefore expected low yet molecular anchoring suited, which may be advantageous for catalytic applications such as methane dry reforming, where similar binding of both gases is needed. On the other hand, binding to VC is rather weak and the material likely unselective: CO_2 physisorption has an E_{ads} of -0.28 eV, comparable to methane interaction of -0.22 eV.

Further better-grounded evaluation of CO_2 selectivity over CH_4 is provided for the temperature range 50–1000 K as based on the estimation of adsorption and desorption rates from harmonic transition state theory (TST) using present DFT-D results, as fully explained in the Supporting Information. Notice that such theoretical approach has been successfully used to explain the experimental biogas upgrading in PMOs.[8] In short, adsorption rates $r_{ads}^{CO_2}$ and $r_{ads}^{CH_4}$ for CO_2 and CH_4 depend on the impingement of molecules on the surfaces and therefore on their partial pressures. Here we evaluate these at two partial pressures, (*i*) 0.01 bar, for capture from dilute streams, *e.g.* coal mine ventilation air with CO_2 and CH_4 contents of 1 v/v % each,[7] and (*ii*) 1.0 bar, to assess gas enrichment at higher pressure, *e.g.* useful for pressure swing adsorption. We refrained the evaluation at higher partial pressures, as model validity could become compromised, see below.

Desorption rates differ for each of the identified sites given in Table 1, but a macroscopic rate is likely superimposed from all contributions, justifying the use of average desorption rates $r_{des}^{CO_2}$ and $r_{des}^{CH_4}$. For their calculation, two different models for entropy losses upon adsorption were devised, accounting for upper and lower limits,[26] which help to rationalize such an effect. In the *hindered model* all translations and rotations are impeded upon adsorption and effectively converted to frustrated vibrations; in the *free model* gas-phase rotational and translational degrees are preserved, the latter in two dimensions above the surface, with the adsorbate fixed only in height. We initially evaluated both models for physisorbed species, namely for CH_4 on all TMCs and CO_2 on VC, though for strongly chemisorbed CO_2 on the other TMCs only the hindered model is considered, being the most likely situation.

To clarify these models, their estimated ad/desorption rates are given in Fig. 2a for TiC (001). Only CO_2 adsorption rates are depicted, as CH_4 ones are simply higher by a factor of 1.7, extracted from the CH_4 smaller molar mass, see Supporting Information. The difference can be considered insignificant within the range of accuracy, though. Larger differing desorption rates are the main factor on selectivity. At intersection points of adsorption and desorption rates one can mark fringe temperatures, above which materials would likely lose their ability to capture significant amounts of CH_4 or CO_2. Taking TiC as an example, see Fig. 2a, one observes that at temperatures below $T_1 = 145$ K and $T_2 = 195$ K CH_4 adsorption rate at 0.01 bar pressure regime is larger than desorption rates, for hindered and free models, respectively. These temperatures rise to $T_3 = 195$ K and $T_4 = 270$ K for the 1.0 bar pressure regime; in all cases, well below ambient temperature; so, CH_4 would not be captured at ambient conditions. Equivalent fringe temperatures are found for ZrC, HfC, NbC, TaC, and VC, as CH_4 desorption rates do not significantly differ, and similar conclusions are extracted.
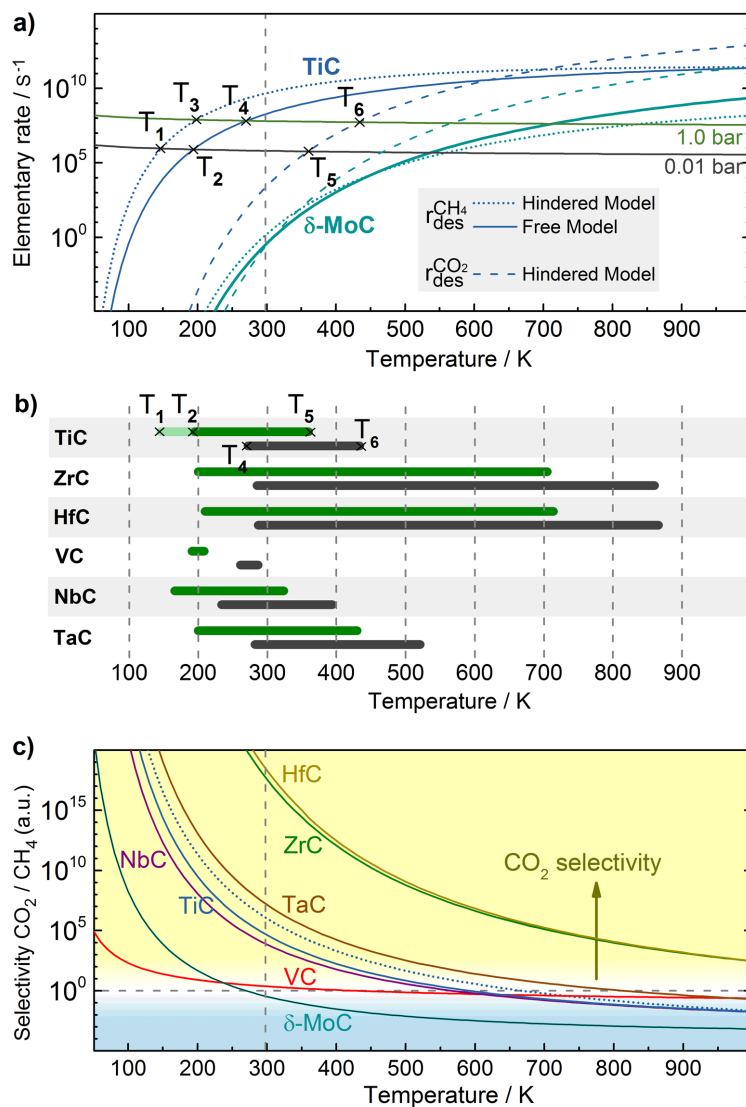
Figure 2. a) Temperature dependence of estimated desorption rates of CO_2 and CH_4 on TiC and δ-MoC (001) surfaces, and adsorption rates for CO_2 at different partial pressures. b) Temperature ranges for different TMC (001) surfaces, where CO_2 adsorption is predicted high with nearly no CH_4 capture. Solid green (dark gray) correspond to partial pressures of 0.01 bar (1.0 bar) evaluated according to free model. Light green gives the hindered model predictions for TiC. c) Temperature dependence of CO_2 selectivity over CH_4 for different TMCs. Solid (dashed) curves correspond to the free (hindered) model. Gray dashed horizontal and vertical lines highlight a selectivity value of 1 and ambient temperature of $T = 298$ K.

For completeness, T_5 = 360 K and T_6 = 435 K mark temperatures below which CO_2 accumulates on TiC at 0.01 and 1.0 bar, respectively, considerably high values that lead us to suggest these materials for CO_2 capture.[13] In combination with fringe CH_4 temperatures T_2 and T_4, lower and higher temperature ends are marked where capture of high amounts of CO_2 with good selectivity over CH_4 are thus predicted. These ranges are graphically depicted in Fig. 2b for all studied TMCs, with the exception of δ-MoC, see below. According to this TiC, NbC, and TaC could be useful around ambient temperatures, whereas ZrC and HfC could be used even at higher temperatures. VC seems hardly usable for such application –as expected from weaker interaction with CO_2– with ranges only given to demonstrate this point. Note that free model values were used in such an analysis, providing the more conservative estimate, yet hindered model would extend the temperature range on the lower end; the example for TiC is provided for 0.01 bar partial pressure. Concerning δ-MoC, CH_4 capture temperature ranges 460 – 520 K at 0.01 bar and 570 – 730 K at 1.0 bar partial pressures, suggest the material for CH_4 capture, in line to previous estimates of ~330 K in vacuum.[21]

Further estimates of low coverage CO_2 selectivity over CH_4, S_{CO_2/CH_4} are obtained for equal CO_2 and CH_4 partial pressures. Selectivity is defined through adsorption/desorption equilibrium constants K_{CO_2} and K_{CH_4}

$$S_{CO_2/CH_4} = \frac{K_{CO_2}}{K_{CH_4}} = \frac{r_{ads}^{CO_2}/r_{des}^{CO_2}}{r_{ads}^{CH_4}/r_{des}^{CH_4}} \qquad (1).$$

Again, S_{CO_2/CH_4} can be evaluated from hindered or free models: A comparison is made for TiC, see Fig. 2c: Hindered model selectivities are ~2 orders of magnitude higher compared to free model values, yet qualitative conclusions remain similar. So, further discussion is restricted to

more conservative free model. Among all studied TMCs, CO_2 selectivity is rather high for TiC, NbC, and TaC and very high for ZrC and HfC, with a wider working temperature range. According to this, selectivity values of 10^5 or higher are predicted even for very low partial pressures of 0.01 bar, which, in theory, ensure a biogas CH_4 enrichment above 99.9%. In contrast, a rather low selectivity is expected for VC and δ-MoC, but the latter does capture both CH_4 and CO_2, interesting for possible use in methane dry reforming at moderate temperatures.

Note that present estimations are given for initial adsorption stages,[8] where adsorbate lateral interactions are disregarded. For CO_2 at medium coverages, these are found not to be repulsive, seen *e.g.* on Ni[27] or α-Mo$_2$C[28] surfaces. For CH_4 pair interactions become increasingly favourable with coverage,[29] *e.g.* in MOF pores[14] or on MgO (001) surface.[29] This effect would decrease CO_2 selectivity at higher pressures. However, CO_2 selectivity is expected to prevail, due to its stronger adsorption.

While keeping these points in mind, a first assessment of the materials CO_2 adsorption capacity seems necessary. Interestingly, this is possible when knowing the specific surface area of a TMC powder sample. We use here a reasonable and conservative estimate of 50 m²/g, justified by values of 450, 200, 140, and 22 m²/g reported by Giordano *et al.*[30] for nanoparticles of VC, TiC, NbC, and Mo$_2$C. For an assumed half monolayer coverage of CO_2 on each TMC surface slab – 2x2 surface slab areas range from 75.0 to 89.1 Å² with in total four CO_2 molecules assumed to be adsorbed–, exemplary capacities of 1.6 to 1.9 wt% are found, comparable in magnitude to 2.2 wt% found at 323 K for MgO with a specific surface area of 32 m^2/g.[31] In combination with the herein demonstrated high CO_2 selectivity over CH_4, specifically synthesized TMC samples exhibiting higher specific surface areas[32] could prove as highly

performing materials. Similar strategies have been successfully applied to significantly increase CO_2 capture capacity on porous MgO samples.[31]

In summary, periodic DFT PBE-D3 calculations on the interaction of CH_4 with most stable (001) surfaces of seven transition metal carbides (TMCs) predict a weak CH_4 attachment for groups 4 and 5 TMCs (TM=Ti, Zr, Hf, V, Nb, Ta) with adsorption energies of ~-0.2 eV, almost exclusively dominated by dispersion. In contrast δ-MoC (group 6) displays a strong interaction with CH_4 of ~-0.8 eV. Comparison to earlier results of strong CO_2 interaction on these materials suggest a highly preferred CO_2 adsorption over CH_4 when TMCs (TM=Ti, Zr, Hf, Nb, Ta, Mo) are exposed to CO_2/CH_4 mixtures. Adsorption and desorption rate estimates mark temperature ranges around ambient conditions (TiC and NbC) or even up to elevated temperatures (ZrC, HfC, and TaC) at which CO_2 capture selectivities above 99.9% are expected even at very low partial pressures, highlighting the usage of such TMCs for CO_2 separation from CH_4 in biogas upgrading.

ASSOCIATED CONTENT

The Supporting Information is available free of charge on the ACS Publications website.

Additional computational details, list of adsorption energies and contributions, and geometric descriptors, top views of ad-sorbate structures, brief explanation of the used rate model.

AUTHOR INFORMATION

Corresponding Author

*francesc.vines@ub.edu

Notes

The authors declare no competing financial interests.

REFERENCES

(1)   Scenario, N. P.; East, M. *World energy outlook 2014*; International Energy Agency (IEA) Publishing, Paris, France, 2014.

(2)   Weiland, P. Biogas Production: Current State and Perspectives. *Appl. Microbiol.*

Biotechnol. **2010**, *85*, 849-860.

(3)   Sun, Q.; Li, H.; Yan, J.; Liu, L.; Yu, Z.; Yu, X. Selection of Appropriate Biogas

Upgrading Technology - A Review of Biogas Cleaning, Upgrading and Utilisation. *Renew.*

Sustain. Energy Rev. **2015**, *51*, 521-532.

(4)   Bae, Y. S.; Snurr, R. Q. Development and Evaluation of Porous Materials for Carbon

Dioxide Separation and Capture. *Angew. Chemie* **2011**, *50*, 11586-11596.

(5)   Freund, H.; Roberts, M. W. Surface Chemistry of Carbon Dioxide. *Surf. Sci. Rep.* **1996**,

25, 225-273.

(6)   Taifan, W.; Boily, J. Surface Chemistry of Carbon Dioxide Revisited. *Surf. Sci. Rep.*

2016, *71*, 595-671.

(7)   Kim, J.; Maiti, A.; Lin, L.-C.; Stolaroff, J. K.; Smit, B.; Aines, R. D. New Materials for

Methane Capture from Dilute and Medium-Concentration Sources. *Nat. Commun.* **2013**, *4*, 1694.

(8)   Kunkel, C.; Viñes, F.; Lourenço, M. A. O.; Ferreira, P.; Gomes, J. R. B.; Illas, F.

Selectivity for CO_2 over CH_4 on a Functionalized Periodic Mesoporous Phenylene-Silica

Explained by Transition State Theory. *Chem. Phys. Lett.* **2017**, *671*, 161-164.

(9)   Ihm, Y.; Cooper, V. R.; Gallego, N. C.; Contescu, C. I.; Morris, J. R. Microstructure-

Dependent Gas Adsorption: Accurate Predictions of Methane Uptake in Nanoporous Carbons. *J.*

Chem. Theory Comput. **2014**, *10*, 1-4.

(10)   González, S.; Viñes, F.; García, J. F.; Erazo, Y.; Illas, F. A DF-vdW Study of the CH_4

Adsorption on Different Ni Surfaces. *Surf. Sci.* **2014**, *625*, 64-68.

(11)   Hao, X.; Wang, Q.; Li, D.; Zhang, R.; Wang, B. The Adsorption and Dissociation of Methane on Cobalt Surfaces: Thermochemistry and Reaction Barriers. *RSC Adv*. **2014**, *4*, 43004-43011.

(12)   Yang, Q.; Liu, D.; Zhong, C.; Li, J. Development of Computational Methodologies for Metal–Organic Frameworks and Their Application in Gas Separations. *Chem. Rev*. **2013**, *113*, 8261-8323.

(13)   Kunkel, C.; Viñes, F.; Illas, F. Transition Metal Carbides as Novel Materials for CO_2 Capture, Storage, and Activation. *Energy Environ. Sci*. **2016**, *9*, 141-144.

(14)   Sillar, K.; Sauer, J. Ab Initio Prediction of Adsorption Isotherms for Small Molecules in Metal–Organic Frameworks: The Effect of Lateral Interactions for Methane/CPO-27-Mg. *J. Am. Chem. Soc*. **2012**, *134*, 18354-18365.

(15)   Srivastava, A.; Chauhan, M.; Singh, R.K. High-Pressure Phase Transitions in Transition Metal Carbides XC (X=Ti, Zr, Hf, V, Nb, Ta): A First-Princple Study. *Phase Transitions* **2011**, *84*, 58-66.

(16)   Porosoff, M. D.; Kattel, S.; Li, W.; Liu, P.; Chen, J. G. Identifying Trends and Descriptors for Selective CO_2 Conversion to CO over Transition Metal Carbides. *Chem. Commun*. **2015**, *51*, 6988-6991.

(17)   Liu, X.; Kunkel, C.; Ramírez de la Piscina, P.; Homs, N.; Viñes, F.; Illas, F. Effective and Highly Selective CO Generation from CO_2 Using a Polycrystalline α-Mo_2C Catalyst. *ACS Catal*. **2017**, *7*, 4323-4335.

(18)   Hwu, H. H.; Chen, J. G. Surface Chemistry of Transition Metal Carbides. *Chem. Rev*. **2005**, *105*, 185-212.

(19)   Levy, R. B.; Boudart, M. Platinum-like Behavior of Tungsten Carbide in Surface Catalysis. *Science* **1973**, *181*, 547-549.

(20)   Tominaga, H.; Nagai, M. Theoretical Study of Methane Reforming on Molybdenum Carbide. *Appl. Catal. A Gen.* **2007**, *328*, 35-42.

(21)   Posada-Pérez, S.; dos Santos Politi, J. R.; Viñes, F.; Illas, F. Methane Capture at Room Temperature: Adsorption on Cubic δ-MoC and Orthorhombic β-Mo_2C Molybdenum Carbide (001) Surfaces. *RSC Adv.* **2015**, *5*, 33737-33746.

(22)   Kresse, G.; Furthmüller, J. Efficient Iterative Schemes for *Ab Initio* Total-Energy Calculations Using a Plane-Wave Basis Set. *Phys. Rev. B* **1996**, *54*, 11169- 11186.

(23)   Perdew, J. P.; Burke, K.; Ernzerhof, M. Generalized Gradient Approximation Made Simple. *Phys. Rev. Lett.* **1996**, *77*, 3865-3868.

(24)   Grimme, S.; Ehrlich, S.; Goerigk, L. Effect of the Damping Function in Dispersion Corrected Density Functional Theory. *J. Comput. Chem.* **2011**, *32*, 1456-1465.

(25)   Boese, A. D.; Sauer, J. Accurate Adsorption Energies for Small Molecules on Oxide Surfaces: CH_4/MgO(001) and C_2H_6/MgO(001). *J. Comput. Chem.* **2016**, *37*, 2374-2385.

(26)   Tait, S. L.; Dohnálek, Z.; Campbell, C. T.; Kay, B. D. n-alkanes on MgO(100). I. Coverage-dependent Desorption Kinetics of n-butane. *J. Chem. Phys.* **2005**, *122*, 164708.

(27)   Wang, S.-G.; Cao, D.-B.; Li, Y.-W.; Wang, J.; Jiao, H. Chemisorption of CO_2 on Nickel Surfaces. *J. Phys. Chem. B* **2005**, *109*, 18956-18963.

(28)   Luo, Q.; Wang, T.; Walther, G.; Beller, M.; Jiao, H. Molybdenum Carbide Catalysed Hydrogen Production from Formic Acid – A Density Functional Theory Study. *J. Power Sources* **2014**, *246*, 548-555.

(29)   Tosoni, S.; Sauer, J. Accurate Quantum Chemical Energies for the Interaction of Hydrocarbons with Oxide Surfaces: CH_4/MgO(001). *Phys. Chem. Chem. Phys.* **2010**, *12*, 14330-14340.

(30)   Giordano, C.; Erpen, C.; Yao, W.; Milke, B.; Antonietti, M. Metal Nitride and Metal Carbide Nanoparticles by a Soft Urea Pathway. *Chem. Mater.* **2009**, *21*, 5136-5144.

(31)   Ding, Y.; Song, G.; Zhu, X.; Chen, R.; Liao, Q. Synthesizing MgO with a High Specific Surface for Carbon Dioxide Adsorption. *RSC Adv.* **2015**, *5*, 30929-30935.

(32)   Flaherty, D. W.; May, R. A.; Berglund, S. P.; Stevenson, K. J.; Mullins, C. B. Low Temperature Synthesis and Characterization of Nanocrystalline Titanium Carbide with Tunable Porous Architectures. *Chem. Mater.* **2010**, *22*, 319-329.

Biogas   Biomethane

CH$_4$/CO$_2$ separation on
transition metal carbides

Ti, Zr, Hf, Nb, Ta

C   O   H